Engineering xxx (xxxx) xxx

Contents lists available at ScienceDirect

Engineering

journal homepage: www.elsevier.com/locate/eng

Views & Comments

# Toward Mobile Satellite Internet: The Fundamental Limitation of Wireless Transmission and Enabling Technologies

Wenjin Wang [a,b,*], Yiming Zhu [a,b], Yafei Wang [a,b], Rui Ding [c], Symeon Chatzinotas [d,*]

[a] National Mobile Communications Research Laboratory, Southeast University, Nanjing 210096, China
[b] Purple Mountain Laboratories, Nanjing 211100, China
[c] China Satellite Network Group Co., Ltd., Beijing 100029, China
[d] Interdisciplinary Centre for Security, Reliability and Trust, University of Luxembourg, Luxembourg L-1855, Luxembourg

ARTICLE INFO

*Article history:*
Received 8 December 2024
Revised 21 April 2025
Accepted 4 July 2025
Available online xxxx

ABSTRACT



## 1. Introduction

It has been almost 60 years since the launch of Intelsat-I, the world's first commercial satellite communications system. Over the past few decades, the development of satellite communications has been driven by both technological advancements and growing application demands, which have given rise to three primary services: broadcast, fixed satellite, and mobile satellite services [1]. Broadcast services, such as those provided by DirecTV and Dish Network, enable the one-way transmission of information to multiple receivers across vast areas. Satellites such as Thaicom-4 and Viasat-3 deliver fixed satellite services, offering broadband access through portable terminals and small ground stations to regions that lack wired or wireless broadband infrastructure. Mobile satellite services, exemplified by providers such as Inmarsat and Iridium, leverage the wide-area coverage of satellites for voice and low-speed data services on handheld terminals, ensuring communication in areas beyond the reach of cellular networks.

Currently, fifth-generation (5G) base stations (BSs) have been widely deployed for cellular mobile communication systems, marking the transition beyond the 5G era. Nevertheless, cellular networks cover less than 40% of the terrestrial surface [2], with only a small fraction of these areas having broadband Internet access for handheld devices through 5G BSs. Consequently, satellite mobile communication is anticipated to play a key role in the evolution of sixth-generation (6G) networks by complementing terrestrial networks (TNs) to provide wireless connectivity with seamless global coverage. To achieve this vision, mobile satellite Internet aims to offer broadband access via portable and ideally handheld devices, further enabling terminal-level integration between TNs and non-terrestrial networks (NTNs). This 6G vision also drives the deployment of cellular radio access networks on satellite regenerative payloads, paving the way for a unified protocol framework. Under this unified framework, the advanced technologies developed for cellular mobile communication systems can be leveraged to satisfy the performance requirements of mobile satellite Internet, while existing cellular infrastructure and economies of scale can be reused to significantly reduce industry costs. However, since cellular protocol frameworks were originally designed for TNs, their applicability to NTNs remains an active area of research, with ongoing efforts underway to develop corresponding technical solutions.

Along with the integration of TNs and NTNs, the selection of appropriate satellite types plays a critical role in enabling ubiquitous connectivity. Low-Earth-orbit (LEO) satellites have emerged as a promising candidate for mobile satellite Internet, owing to the low launch cost, transmission latency, and path loss enabled by their low orbital altitude. However, while the low orbital altitude of LEO satellites offers these advantages, it also limits the coverage area of individual satellites and shortens the visibility duration over given locations, thereby necessitating the deployment of ultra-dense constellations to achieve seamless global coverage. In recent years, advancements in LEO satellite manufacturing and reusable launch vehicle technologies have stimulated the emergence of LEO mega-constellations, driving significant engineering efforts and commercial innovations in mobile satellite Internet [3]. A prominent example is SpaceX's Starlink, which aims to deploy over 42 000 LEO satellites on several

* Corresponding authors.
*E-mail addresses:* wangwj@seu.edu.cn (W. Wang), symeon.chatzinotas@uni.lu (S. Chatzinotas).

https://doi.org/10.1016/j.eng.2025.07.007


Please cite this article as: W. Wang, Y. Zhu, Y. Wang et al., Toward Mobile Satellite Internet: The Fundamental Limitation of Wireless Transmission and Enabling Technologies, Engineering, https://doi.org/10.1016/j.eng.2025.07.007

different orbit altitudes to provide global broadband Internet services [1]. In December 2024, SpaceX completed Starlink's first direct-to-cell (DTC) LEO constellation, enabling unmodified fourth-generation (4G) long term evolution (LTE) handheld terminals to achieve Internet connectivity in remote areas [4].

In addition to being driven by demand and technology, the engineering and commercialization of satellite communication systems are constrained by manufacturing capabilities and costs due to the inherent characteristics of satellite communication, which include long-distance radio propagation and limited onboard power. When discussing the engineering development of satellite communications, starting from the mathematical essence of satellite-to-ground wireless transmission provides valuable insights into the fundamental limitations and potential avenues for transmission capability improvement. By assessing the tradeoffs between the performance gains provided by technologies and their engineering feasibility, alongside commercial costs, it is possible to critically evaluate existing advancements and conceptualize enabling technologies for mobile satellite Internet.

## 2. Fundamental limitations

While the radio propagation distance of terrestrial cellular communications is typically less than 10 km, satellite-to-ground link distances range from 300 to 36 000 km, resulting in significantly larger path loss in satellite-to-ground radio propagation. From both engineering and commercial perspectives, launch capability and system costs impose strict constraints on the size of solar panels, volume of onboard batteries, and aperture of payload antennas. Furthermore, the batteries and antennas of user terminals (UTs) must be integrated into a compact design to fulfill portability requirements. These inherent characteristics of satellite mobile communication systems significantly affect the performance of satellite-to-ground downlink (DL) and uplink (UL) radio transmissions, which is shown in Fig. 1. As a representative case, we focus on the DL transmission for analysis, which can be captured by the following link budget formula [5,6]:

$$R_{\mathrm{b}} = \alpha \frac{(\mathrm{EIRP})_{\mathrm{sat}} \cdot (G/T)_{\mathrm{ue}}}{f^2 \cdot d^2 \cdot (E_{\mathrm{b}}/N_0)_{\mathrm{req}}} \tag{1}$$

where $R_{\mathrm{b}}$ is the DL transmission rate; $(\mathrm{EIRP})_{\mathrm{sat}}$ represents the effective isotropic radiated power (EIRP) of payloads; $(G/T)_{\mathrm{ue}}$ denotes the antenna gain to noise–temperature ratio ($G/T$) of UTs; $f$ and $d$ refer to the carrier frequency and satellite-to-ground distance, respectively; and $(E_{\mathrm{b}}/N_0)_{\mathrm{req}}$ indicates the minimum energy per bit to noise power spectral density ratio required for demodulation with a specified bit error rate (BER), where $E_{\mathrm{b}}$ and $N_0$ denote energy per bit and noise power spectral density, respectively. In addition, the constant $\alpha$ can be expressed as $\alpha = c^2/(16\pi^2 \cdot k \cdot M)$, where $k$, $c$, and $M$ denote the Boltzmann constant, light speed, and link margin, respectively. In practice, based on the characteristics of satellite-to-ground wireless channels, it is necessary to reserve the link margin $M$ to account for other losses, including the atmospheric absorption, rain and cloud attenuation, scintillation loss, feeder loss between transceivers and antennas, antenna pointing loss, interference, and so on [5,6]. Atmospheric absorption, rain and cloud attenuation, and tropospheric scintillation are relatively significant at higher frequencies, while ionospheric scintillation primarily impacts the sub 6 GHz band. It is worth noting that the value of the link margin $M$ plays an important role in the tradeoff between spectral efficiency and reliability.

Consequently, the satellite-to-ground wireless transmission rate is determined by the EIRP of payloads $(\mathrm{EIRP})_{\mathrm{sat}}$, $G/T$ of UTs $(G/T)_{\mathrm{ue}}$, carrier frequency $f$, satellite-to-ground distance $d$, and demodulation threshold $(E_{\mathrm{b}}/N_0)_{\mathrm{req}}$. Notably, due to the large propagation delay, the automatic retransmission mechanisms commonly used in TNs are difficult to implement in NTNs. As a result, it is generally necessary to reserve a higher modulation and demodulation margin to ensure reliable communication. This simple formula thus establishes a fundamental connection between the theoretical rate of the satellite-to-ground DL and the engineering design. The same principle also applies to the UL of satellite-to-ground communication.

### 2.1. Payloads

The EIRP of the payload is defined as the product of the transmit power and the antenna gain. The transmit power of the payload depends on the satellite's power-supply system, which typically includes solar panels that convert solar energy into electrical power and onboard batteries that store energy to ensure a contin-

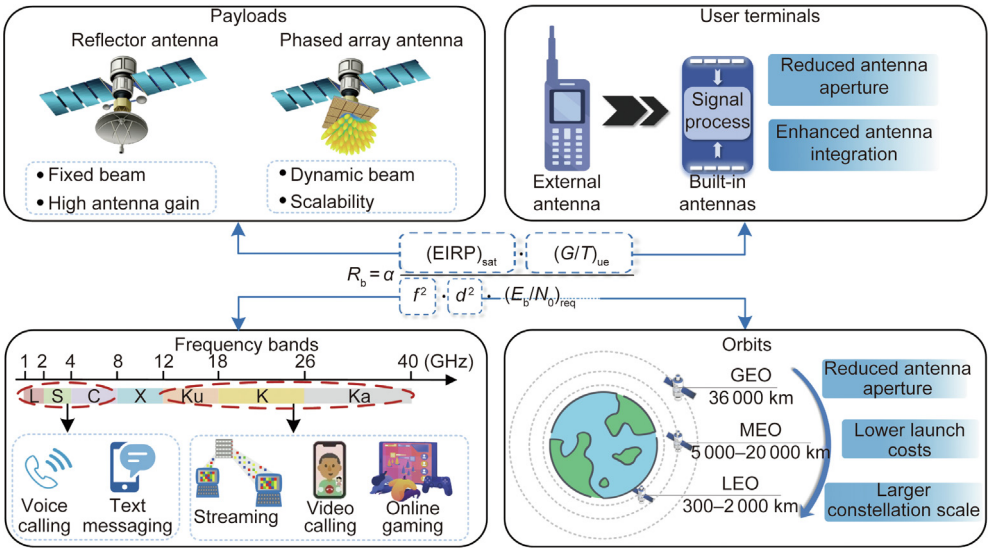


**Fig. 1.** Fundamental limitations of mobile satellite Internet. MEO: medium Earth orbit; GEO: geostationary Earth orbit; $R_{\mathrm{b}}$: DL transmission rate; $\alpha$: constant; $(\mathrm{EIRP})_{\mathrm{sat}}$: effective isotropic radiated power of payloads; $(G/T)_{\mathrm{ue}}$: antenna gain to noise–temperature ratio ($G/T$) of UTs; $f$: carrier frequency; $d$: satellite-to-ground distance; $(E_{\mathrm{b}}/N_0)_{\mathrm{req}}$: minimum energy per bit to noise power spectral density ratio required for demodulation with a specified bit error rate; $E_{\mathrm{b}}$: energy per bit; $N_0$: noise power spectral density.

uous power supply during periods without sunlight. On the other hand, the transmit antenna gain of the payload is directly proportional to the size of the antenna aperture. A larger aperture allows for more focused emission of radiated energy in a particular direction.

In addition to gradual improvements in EIRP with the development of industrial capabilities, the innovation of multi-beam technology has become the primary driving force behind the significant increase in payload capacity, leading to the emergence of high-throughput satellites. By using reflector antennas with multiple feeds or phased-array antennas with analog/digital beamforming, numerous high-gain beams can be generalized on a single antenna aperture [7]. Although the EIRP of a single beam is not significantly improved, and may even slightly decrease compared with a wide beam, due to the distribution of power across multiple beams, the capacity of a payload increases by orders of magnitude through spatial division multiplexing and frequency spectrum reuse.

Under the constraints of manufacturing processes, increasing either the satellite's EIRP or the number of beams inevitably requires an increase in the satellite's volume, weight, and cost. Once the critical threshold of industrial capacity is exceeded, the cost will increase dramatically beyond affordability. In addition, to mitigate interference from non-geostationary satellite networks to other systems, regulatory bodies such as the International Telecommunication Union (ITU) have established constraints on the power-flux density (PFD), which means that the EIRP cannot be arbitrarily increased [8].

### 2.2. User terminals

The DL transmission rate increases linearly with the $G/T$ of UTs, which is determined by the noise figure and receiving antenna gain. Specifically, integrating high-performance, low-noise components can minimize noise contributions to subsequent stages, while exploiting larger aperture antennas in UTs can increase the antenna gain. The overall noise figure of the receiver system is dominated by the first active module—that is, the low-noise amplifier. With advancements in semiconductor materials and processes, the noise figure of low-noise amplifiers in UTs has significantly decreased, reaching minimum values below 1 dB [9]; thus, there is limited potential for further reduction. Nevertheless, the market demand increasingly emphasizes the portability of UTs, driving the miniaturization and internal integration of UT antennas. These antennas have evolved from external linearly polarized antennas used in dedicated satellite phones to multiple internally integrated antennas within modern smartphones [10]. However, the limitation on terminal size imposes significant restrictions on the antenna aperture, making it increasingly challenging to increase the $G/T$ value of UTs and calling for a more advanced UT antenna design. Meanwhile, beam-management strategies for UTs equipped with multiple antennas require dedicated design. A simple and effective solution at the receiver side is to perform directional receive beamforming steered toward the serving satellite.

### 2.3. Frequency bands

As shown in Eq. (1), higher operating frequencies result in a reduction in user data rates. To effectively leverage the large bandwidth available in high-frequency bands, such as the Ka-band, for broadband access, it is essential to significantly improve the EIRP and the $G/T$ to mitigate the adverse effects of higher carrier frequencies on data rates. Consequently, satellite terminals operating in the Ka/Ku bands commonly utilize parabolic reflectors or phased arrays. However, the high cost and limited portability of these larger terminals hinder widespread user adoption, rendering them less suitable for mobile satellite Internet services.

Compared with the Ku/Ka bands, the L/S bands offer superior signal penetration and broader coverage, significantly easing the hardware requirements for UTs. These favorable propagation characteristics not only enable NTNs to support reliable outdoor connectivity but also make lightweight indoor connectivity feasible, such as in vehicles or near windows. Since services such as voice communications demand limited spectral resources but require highly compact terminal designs, the L/S bands have become the preferred choice for narrowband satellite mobile communication services. Given the similarity of L/S bands to the frequency bands used by terrestrial cellular networks, L/S bands can be more readily integrated into unified terrestrial terminals utilizing similar or even unified communication protocol frameworks [11]. This greatly expands the potential to increase the number of users. However, aside from a small portion of sub-6 GHz spectrum allocated to satellite operators, the vast majority of sub-6 GHz spectrum resources are already occupied by terrestrial operators, making it difficult to accommodate the growing spectrum demands of the future mobile satellite Internet. As satellites typically aim to provide service in areas not covered by cellular networks, they may reuse terrestrial frequency bands without interference in order to efficiently alleviate bandwidth scarcity in lower frequencies. Consequently, the spectrum sharing of sub-6 GHz bands between TNs and NTNs is a potential pathway for future mobile satellite networks.

Given the anticipated trend of TN–NTN integration in 5G/6G and the frequency band limitations encountered by satellites, spectrum sharing in TN–NTN coexistence scenarios has become an important topic worthy of attention. When the service areas of TNs and NTNs are geographically separated, mutual interference can be considered negligible. Therefore, most existing studies on spectrum sharing primarily focus on scenarios where TN and NTN coverage areas overlap. Most satellite systems adopt the frequency-division duplexing (FDD) mode, in which the NTN UL or DL can share a spectrum with the TN FDD UL, DL, or time-division duplexing (TDD) bands.

From the UL/DL perspective [12], different sharing modes lead to distinct interference patterns. When an NTN DL shares a spectrum with a TN DL, the NTN users are typically located outside the coverage area of terrestrial BSs; thus, only interference from the satellites to the TN users needs to be mitigated. In the case of an NTN DL sharing with a TN UL, satellite-side spectrum sensing can be employed to identify spectrum opportunities in the TN UL, thereby avoiding excessive interference. When an NTN UL overlaps with a TN DL, the highly directional downward beamforming of terrestrial BSs typically results in negligible interference to satellites. However, an NTN UL sharing with a TN UL is generally infeasible, as significant mutual interference arises from the wide sidelobes of UT antennas in both systems.

From the perspective of TDD/FDD [13], spectrum sharing between NTNs and FDD-based TN systems can be configured in either normal or reverse pairing modes. In reverse pairing, the NTN UL and DL share a spectrum with the TN DL and UL, respectively; in normal pairing, both the NTN and TN use the same UL and DL frequency bands. Compared with normal pairing, reverse pairing offers improved interference mitigation due to the differing beam directions between the two networks. For spectrum sharing between an NTN and a TDD-based TN, although the TN UL and DL share the same frequency band, the NTN UL and DL can still operate in an FDD mode over distinct TDD carriers typically available in the TN, making spectrum sharing feasible. In this case, based on the analysis of the UL/DL perspective, more sophisticated interference mitigation techniques are required in TDD-based TNs to ensure reliable communication, as both the TN UL and DL coexist in the shared band.

To manage these coexistence challenges, spectrum-sharing strategies are generally categorized as either static or dynamic. Static schemes, such as the seven-color reuse approach, employ predefined frequency division to separate TN and NTN users in overlapping areas. While these schemes offer advantages in terms of engineering deployment, they fall short in enabling real-time and efficient spectrum utilization. More advanced static methods include exclusion zone-based protection, which involves establishing protective regions across multiple dimensions, such as frequency bands, geographic locations, and spatial angles [14]. In contrast, dynamic sharing schemes, such as overlay, underlay, and hybrid approaches [15], leverage spectrum sensing and cognition radio technologies for adaptive access to shared frequency bands. Complementary techniques such as joint user scheduling [16], beamforming, and waveform design [17] can further enhance coexistence performance. However, aside from conventional static spectrum-sharing schemes, most advanced approaches require substantial protocol modifications and extensive inter-network information exchange, which pose major barriers to practical deployment.

### 2.4. Orbits

Eq. (1) also reveals the impact of orbital altitude on the data rate. Specifically, if the orbital altitude is halved, the antenna aperture required to achieve the same data rate can be reduced to a quarter of its original size, thereby significantly lowering manufacturing and launch costs. However, a decrease in orbital altitude also reduces the coverage area of individual satellites, which necessitates the deployment of larger constellations to achieve global coverage. Moreover, a lower orbital altitude results in a higher satellite velocity, leading to a shorter satellite pass time overhead and requiring more frequent handovers. Therefore, selecting the optimal orbit altitude involves balancing satellite costs against the constellation scale, leading satellite operators to make different choices based on their technical capabilities and commercial considerations. For example, Starlink's satellites at an altitude of approximately 350 km provide DTC services using a mega constellation with relatively small antenna apertures. In comparison, AST SpaceMobile employs a small-scale constellation with much larger antenna apertures at an altitude of approximately 700 km.

### 2.5. Waveforms

The demodulation threshold $(E_b/N_0)_{req}$ in Eq. (1) captures the impact of waveform design on the satellite-to-ground transmission rate, since different waveforms exhibit distinct BER curves with respect to $E_b/N_0$, resulting in varying $(E_b/N_0)_{req}$ for a given spectral efficiency and reliability requirement. Although the protocol design and physical-layer technologies of cellular mobile communication systems work well in TNs, they are not directly applicable to satellite communications because of the unique characteristics of satellite-to-ground channels. Thus, modifications to existing protocol frameworks and the development of NTN physical-layer technologies are required for mobile satellite Internet.

In mobile satellite Internet, satellite-to-ground channels change continuously due to various propagation impairments, including atmospheric absorption, scintillation disturbances, interference, and the relative motion between satellites and ground terminals [5], resulting in dynamic large-scale fading. In addition, cellular terminals are typically equipped with the limited number of omnidirectional antennas, leading to relatively poor antenna directivity. Consequently, multipath effects, caused by signal reflections from the ground and surrounding obstacles, become non-negligible when mobile satellite Internet provides broadband access to cellular terminals [5]. The combined effect of large-scale and multipath fading further exacerbates the dynamic fluctuations of the received $E_b/N_0$, leading to degraded link stability and reduced spectral efficiency. To address these challenges, the adaptive modulation and coding (AMC) technique can be adopted to balance reliability and spectral efficiency by adaptively adjusting the modulation and coding schemes (MCSs) based on real-time channel conditions. Specifically, the UTs select an appropriate MCS level with a specified demodulation threshold $(E_b/N_0)_{req}$, based on an estimation of the received $E_b/N_0$ [18]. The selected MCS level is then fed back to the satellites via the channel quality indicator (CQI), enabling the transmitter to adjust its MCSs accordingly. Conversely, in the absence of AMC, the satellites must conservatively select the MCS level with a low demodulation threshold $(E_b/N_0)_{req}$, based on worst-case channel conditions to ensure link reliability. While this conservative strategy guarantees robustness, it results in inefficient power utilization and limits the achievable data rate under favorable channel conditions.

Apart from large-scale fading and multipath effects, the high relative velocity between the satellite and the UT induces large dynamic Doppler shifts, while the long transmission distance results in long dynamic propagation delays. For instance, a LEO satellite at an altitude of 600 km operating at 2.6 GHz will experience a minimum one-way propagation delay of up to 2 ms and a Doppler shift exceeding 50 kHz. Long dynamic propagation delays render timing and retransmission mechanisms inefficient or even inoperable. The timing mechanisms defined in cellular systems are not designed to accommodate such large and rapidly changing delays, resulting in increased interference and even the failure of random access or UL transmission. To address this issue, it is necessary to redesign the timing mechanism by incorporating preamble, ephemeris data, and global navigation satellite system (GNSS) information to ensure reliable synchronization for mobile satellite Internet [19]. Regarding the retransmission mechanism, the long propagation delays significantly extend the duration of each hybrid automatic repeat request (HARQ) process, particularly when errors occur, causing HARQ resource depletion and reduced transmission efficiency. Given the limited number of HARQ processes, one feasible solution is to disable HARQ feedback in order to eliminate the extended stop-and-wait delays at the sacrifice of reduced link reliability [11]. This would ultimately necessitate a higher demodulation threshold $(E_b/N_0)_{req}$ compared with cellular mobile communication systems. In addition to long propagation delays, large dynamic Doppler shifts present a major challenge, as they severely degrade the performance of orthogonal frequency-division multiplexing (OFDM)—the primary waveform employed in mobile satellite Internet. More specifically, they can disrupt the orthogonality among subcarriers and even cause subcarrier misalignment, resulting in inter-carrier interference (ICI) and degraded demodulation accuracy. Therefore, accurate timing and frequency offset estimations using DL synchronization signals under large dynamic Doppler shifts [20] are essential to improve the subsequent demodulation performance of receivers in mobile satellite Internet.

## 3. Enabling technologies

### 3.1. Extremely large antenna arrays

In the user links of mobile satellite Internet, extremely large antenna arrays (ELAAs) are one of the most promising technologies for enhancing satellite-to-ground transmission performance [7], which is shown in Fig.2. By leveraging beamforming techniques, ELAAs can dynamically generate numerous high-gain narrow beams, thereby improving the EIRP of payloads and increasing spatial multiplexing capabilities. The antenna gain of a satellite ($G_{sat}$)

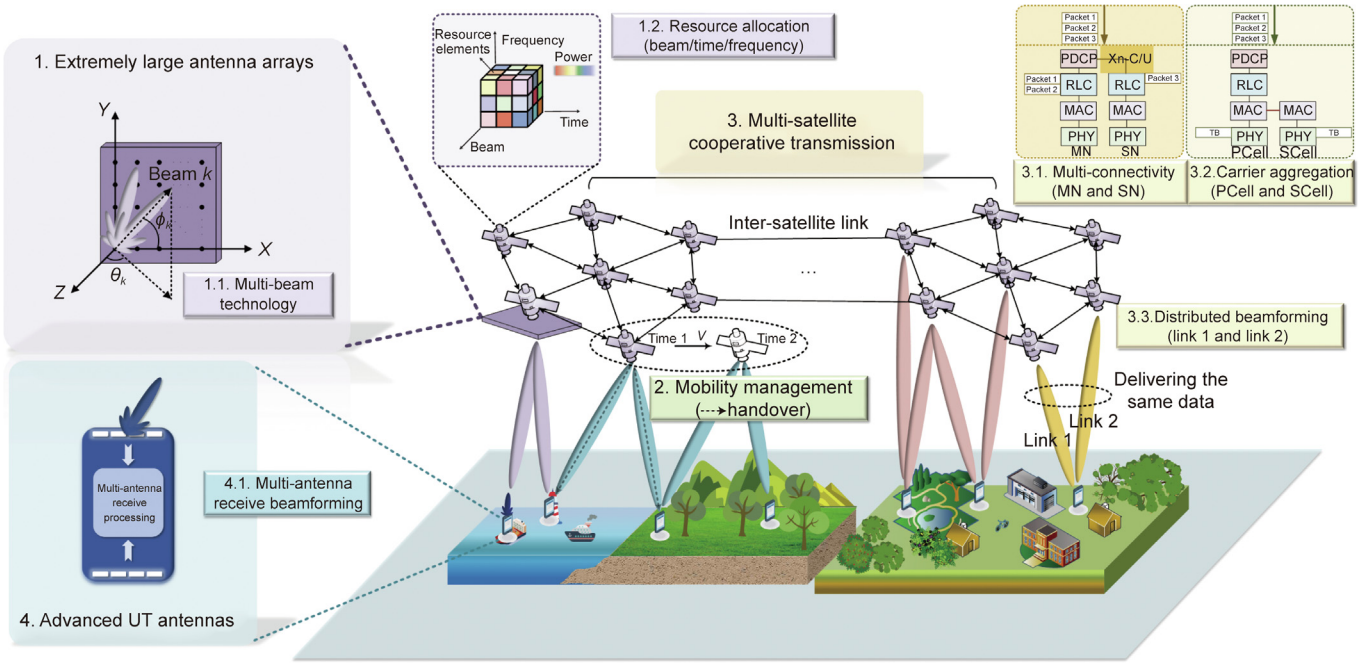


**Fig. 2.** Enabling technologies for mobile satellite Internet. $\phi_k$: the angle between the beam direction and the *X*-axis; $\theta_k$: the angle between the beam direction projected in the *X*–*Z* plane and the *Z*-axis; *V*: velocity; *X*, *Y*, and *Z*: axes in cartesian coordinate system; PDCP: packet data convergence protocol; RLC: radio link control; MAC: medium access control; PHY: physical; MN: master node; SN: secondary node; TB: transport block; PCell: primary cell; SCell: secondary cell; Xn C/U: Xn-control plane/Xn-user plane.

can be quantitatively expressed as $G_{\text{sat}} = \eta 4\pi A f^2/c^2$ [21], where $\eta$ represents the aperture efficiency and $A$ denotes the physical aperture area. This relationship reveals that the antenna gain increases with both the aperture area and the square of the operating frequency. In practical systems, the satellite volume imposes strict constraints on the allowable antenna aperture. These limitations reflect a fundamental tradeoff between performance, volume, and cost, capping the maximum feasible antenna gain achievable through aperture enlargement. Given these constraints, increasing the operating frequency becomes an effective means to increase antenna gain without enlarging the antenna size. For instance, the experimental satellite BlueWalker 3 of AST SpaceMobile requires a 64 $m^2$ ELAA to provide DTC services for handheld terminals operating in the 800 MHz band [22]. If the same gain was to be achieved at 2 GHz, the required aperture area could be reduced to approximately 10.24 $m^2$, highlighting the substantial size savings enabled by higher frequencies. Nevertheless, this gain advantage is exactly counterbalanced by the corresponding increase in free-space path loss, which also grows proportionally to the square of the frequency. This implies that simply increasing the frequency does not lead to improvement in the received signal power under fixed aperture constraints.

Beamforming is a key enabler for unlocking the potential of ELAAs in mobile satellite Internet. Among various types, beam pattern-oriented beamforming is the most widely adopted in current practical satellite communication systems. It relies on channel state information (CSI)-independent predefined beams that can be jointly optimized with beam-scheduling combination in the design stage to mitigate inter-beam interference, and includes Earth-moving and Earth-fixed designs. The former uses static codebooks (e.g., discrete Fourier transform (DFT)-based codebooks) to steer beams relative to the satellite, whereas the latter dynamically focuses the signal energy toward predefined beam locations using real-time geographic information [23]. Beam pattern-oriented beamforming has become a focal point in practical system implementation due to its low computational complexity and reduced reliance on real-time CSI.

In contrast, user-specific beamforming dynamically designs beamforming vectors based on user CSI to increase the received power and suppress interference. While maximum radio transmission (MRT) provides low-complexity solutions, zero forcing (ZF) and minimum mean squared error (MMSE) involve matrix inversion for more effective interference management, and weighted MMSE (WMMSE) further improves the sum-rate performance through iterative optimization. However, user-specific beamforming in satellite communication scenarios presents two major challenges: accurate CSI acquisition and computational complexity. To alleviate instantaneous CSI dependence, several beamforming strategies based on statistical channel characteristics have been proposed, including average power and angles of departure, to maximize the average signal-to-interference and noise ratio (SINR) [24]. To address the computational complexity issue introduced by large antenna dimensions, the application of beam-domain linear precoding on top of Earth-moving beamforming has emerged as a promising transmission architecture for suppressing inter-beam interference in large-scale systems [23]. From the perspective of hardware architecture, given the computational capacity constraints of satellites, analog beamforming—characterized by low computational complexity, reduced analog-to-digital (AD) and digital-to-analog (DA) conversion requirements, and lower demands on digital interface capacity—may serve as a transitional approach. As satellite computational capabilities continue to improve, digital beamforming is emerging as a promising alternative due to its flexibility; however, it remains limited by the number of beams required for full-area coverage.

While beamforming design can significantly increase spatial division gains, intra- and inter-satellite co-channel interference cannot be fully mitigated. Moreover, the traffic demand in mobile satellite Internet systems is typically non-uniform and time-varying [25]. It should be noted that the link budget analysis in this work primarily focuses on point-to-point communication rates. When extended to power-constrained multi-user transmissions over the multiple domains of time, frequency, and space, the overall system throughput becomes increasingly sensitive to the

resource-allocation strategies employed. This sensitivity is further amplified in ELAA-based systems, where beam energy is highly concentrated and the number of simultaneous beams is limited, making efficient resource allocation crucial. As satellite systems scale toward LEO mega-constellations, the resource-allocation problem is growing increasingly high-dimensional and interdependent, emphasizing the importance of low-complexity and cooperative solutions. A key technique for improving resource-management flexibility is service-oriented beam hopping, which selectively activates beams in different time slots based on user distribution and service demand. When jointly optimized with frequency and power allocation, such beam-hopping techniques enable efficient multi-dimensional resource-allocation optimization, thereby supporting diverse service demands such as quality of service (QoS) and energy efficiency [26].

### 3.2. Mobility management

Mobility management is a vital aspect of mobile satellite Internet and presents unique challenges compared with the management of terrestrial systems. From the perspective of broadband transmission for handheld terminals, satellites are typically equipped with ELAAs, which generate narrow beams. As a result, the number of beam footprints significantly exceeds the number of simultaneously active beams, requiring dynamic beam scheduling to ensure effective coverage of specific areas or users. From the perspective of a dense LEO network, the small coverage area and rapid movement of LEO satellites cause frequent handovers as users are served by rapidly shifting narrow beams from different satellites, underscoring the importance of efficient mobility management. Against this backdrop, handover strategies are particularly critical [27]. Specifically, conditional handover and multi-connectivity (MC) [28] respectively increase the robustness of the handover process by preparing possible connections in advance and maintaining multiple connections simultaneously. Beyond seamless handover, multiple users can be grouped for simultaneous handover between satellites, further alleviating the additional signaling overhead. Mobility management must address interdependent high-dimensional optimization challenges, similar to those in resource allocation, while accounting for diverse service requirements, making it increasingly complicated to design tailored handover strategies.

Measurement is the foundation of mobility management in the mobile satellite Internet. A typical approach involves periodic CSI estimation, including channel gain, fading characteristics, and interference levels, as well as mobility-related metrics such as handover frequency, success rate, and latency. Given the narrow beams generated by ELAAs, it is essential to design mobility-management-oriented beam-hopping schemes during the measurement phase to ensure that appropriate beams are aligned with terminals for accurate assessment. Beyond real-time CSI measurements, satellite ephemeris and user-reported location data enable the acquisition of the geographic positions of both transmitters and receivers—a fundamental and inherent advantage of NTNs over TNs. By jointly leveraging both beam-level measurement-oriented beam hopping and location information, more effective mobility measurement strategies can be developed. For example, beam resources can be scheduled based on the geographic locations of users to enable measurements for mobility-related tasks such as handover, thereby increasing the efficiency of beam resource utilization.

### 3.3. Multi-satellite cooperative transmission

In high-density LEO mega constellations such as Starlink, users in most areas typically have access to a substantial number of satellites. These satellites can share information through inter-satellite links (ISLs), enabling cooperative transmission and resource aggregation to serve users within their overlapping coverage areas. Such a transmission mechanism holds significant potential to distribute traffic, balance load, and improve both peak rates and reliability, making it a promising technology to realize the vision of the mobile satellite Internet. We examine multi-satellite cooperation transmission (MSCT) from two perspectives: cooperation modes and computational architectures. More specifically, we categorize cooperation modes into spatial domain, time–frequency domain, and multi-domain cooperation, each with distinct design characteristics, advantages, and limitations. In addition, we emphasize the critical role of the computational architecture in the practical implementation of multi-satellite cooperation. It is worth noting that different cooperation methods impose varying requirements on the computational architecture. Even within the same cooperation strategy, multiple architectures may coexist to accommodate diverse performance tradeoffs.

Spatial-domain cooperation refers to the joint design of beamforming or precoding schemes across multiple satellites to increase the link budget by increasing the transmit power, suppressing interference, or enabling spatial multiplexing. A straightforward approach for cooperative transmission involves delivering a user's DL data stream through coherent DL beamforming from multiple satellites, effectively combining their antenna apertures into a cell-free multiple input multiple output (MIMO) [29]. This technique, known as distributed beamforming (DB) in cellular communications, takes advantage of both the larger antenna gain and additional transmit power, increases the EIRP, and thus improves the achievable data rate. However, this potential performance gain cannot be fully exploited unless the real-time channel phases of all satellite-to-ground links are perfectly known at the transmitters and the delay differences between the links are perfectly pre-compensated for, which would scarcely be possible in fast-moving LEO satellite constellations. While achieving higher antenna gain through an increased aperture is challenging, aggregating transmit power across multiple satellites remains possible as a way to increase the overall signal strength and improve achievable data rates. Therefore, further analysis is required to understand the limits of DB gain under imperfect CSI.

In contrast, receive-side spatial multiplexing is a non-coherent strategy in which different satellites transmit distinct data streams to a UT equipped with multiple antennas to separate them by angle of arrival [30]. While this method increases the number of data streams and avoids stringent inter-satellite synchronization, it imposes hardware complexity at the user side, particularly for handheld terminal, and may suffer from inter-stream interference. Both strategies require the exchange of CSI, joint beamforming design, and resource-allocation information among satellites, necessitating both physical-layer support via ISLs and higher-layer coordination mechanisms, such as the MC mechanism specified in the 3rd Generation Partnership Project (3GPP) NTN specifications [11]. With respect to satellite types, swarm-based cell-free MIMO has emerged as another promising approach for multi-satellite cooperation [31]. This approach leverages constellations composed of small satellites rather than conventional co- or cross-orbit configurations. These systems can employ either wired or wireless ISLs, allowing extremely short inter-satellite distances (on the order of meters), which greatly simplifies synchronization and coordination. However, the close physical proximity of antennas may limit spatial multiplexing gains at the transmitter.

Time–frequency domain cooperation involves splitting or duplicating user data across multiple satellites operating over orthogonal time–frequency resources. This approach enables increased throughput for high-demand users or improved performance for edge users. A representative technique in time–frequency domain cooperation is carrier aggregation (CA) [32], which allows a termi-

nal to simultaneously access multiple carriers from one or more satellites. This significantly reduces the inter-satellite signaling overhead and leverages well-established technologies developed for LTE and beyond [33]. However, its implementation requires wide spectrum availability and imposes stricter hardware constraints at the receiver side, which limit its suitability for resource-constrained terminals. Since the DL of satellite mobile communications is power-limited, it is challenging for a single satellite to support high spectral efficiency using higher-order modulation and high-rate channel coding. Although frequency division multiplexing does not increase the total bandwidth compared with a single satellite using the entire spectrum, the power aggregated from multiple satellites can still result in a proportional improvement in the data transmission rate. The spatial division multiplexing technique requires the incorporation of multiple beams generated by multiple antenna terminals, as will be discussed in the next subsection. Moreover, MC can be regarded as a time–frequency domain cooperation approach and is well suited for practical engineering deployment [34], similar to CA. The inter-satellite information exchange of CA and MC both rely on the Xn interface, which connects two satellites to support control and user plane signaling through ISLs. For CA, the terminal only establishes a radio resource control (RRC) connection with the primary cell, and the data packets for the multi-satellite system are split and aggregated at the medium access control (MAC) layer. In contrast, in MC, the terminal establishes RRC connections with both master-node and second-node satellites [11,34], and data is split and aggregated at the packet data convergence protocol (PDCP) layer. This results in higher signaling overhead in MC but enables the terminal to pre-establish RRC connections with satellites, facilitating seamless handover. The differences in data splitting and aggregation processes between the MAC and PDCP layers lead to varying granularity in resource allocation for CA and MC.

Multi-domain cooperation refers to integrated schemes that jointly coordinate spatial, temporal, and frequency resources among satellites to achieve both orthogonal and coherent transmissions. This cooperation mode theoretically offers optimal performance, but it also imposes stringent requirements on inter-node synchronization, communication latency and capacity, and the computational complexity of the cooperation algorithms. A representative example is coordinated multi-point (CoMP) transmission [35], which was originally developed for TNs. It supports various modes, including cooperative resource allocation, coordinated beamforming, or a combination of both. Although CoMP has been well-studied in TNs, its adaptation to mobile satellite Internet is still required in order to address the unique characteristics of NTNs. Additionally, since MC enables inter-satellite cooperation at higher protocol layers, it can also serve as a foundation for other MSCT methods. In this sense, it can also be regarded as a form of multi-domain cooperation.

The computational architecture that supports MSCT is closely intertwined with engineering implementation. The most fundamental form is fully centralized processing, in which a master satellite coordinates all transmission decisions. While this architecture can achieve optimal performance, it places the heavy computational burden on the master node and often requires significant real-time inter-satellite data exchange. An alternative approach involves distributing specific tasks to secondary nodes, such as large-scale fading precoding/decoding [36] or different levels of cooperative processing, as discussed in Ref. [37]. These architectures alleviate computational pressure, reduce signaling overhead, and offer better scalability. Different cooperation levels demand varying computational capacities, real-time responsiveness, and volumes of inter-satellite data exchange, making the architectural choice critical to system feasibility and performance.

### 3.4. Advanced UT antennas

One of the key technical challenges in mobile satellite Internet is to provide broadband access via handheld terminals. Early dedicated satellite handheld terminals predominantly employed external antennas with linear or circular polarization to achieve high gain [38], but such designs were often bulky, visually obtrusive, and susceptible to mechanical damage. To overcome these limitations, two representative designs have emerged: those that integrate a dedicated high-gain satellite antenna within the device; and those that reuse existing cellular MIMO arrays through beamforming techniques. Both approaches reflect the ongoing shift toward compact and internally integrated antenna solutions for handheld terminals to support mobile satellite Internet.

The first approach involves deploying a single high-gain dedicated satellite antenna by designing a highly directional antenna pattern, along with filtering and impedance-matching networks to isolate different signals without sacrificing compactness [39]. For example, the Huawei Mate 60 Pro smartphone, released in 2023, incorporates a high-gain dedicated satellite antenna within its all-metal bezel to establish connections with geostationary satellites. It should be noted that the direction of this antenna pattern is fixed relative to the handheld terminal, requiring manual adjustment to point toward the satellite, which inherently limits operational flexibility. The second approach leverages existing sub-6 GHz MIMO cellular antennas in modern smartphones for satellite communications through beamforming techniques [30]. This approach aligns with the development of integrated satellite–terrestrial networks, which encourages hardware reuse between cellular and satellite systems. Compared with the dedicated-antenna approach, the MIMO-based method provides greater flexibility and compatibility with existing mass-market hardware.

Overall, both approaches reflect the ongoing trend toward highly integrated, compact, and multi-antenna satellite handheld terminals. Multi-antenna terminals can utilize location information or reference signals to acquire accurate angle estimation, facilitating automatic and continuous alignment of the receiving beam with the satellite. Consequently, these terminals can generate multiple receiving beams to enable the reception of identical or distinct data streams from multiple satellites, thereby providing diversity or multiplexing gains. Despite these potential advantages, practical challenges remain for multi-antenna terminals. One significant issue is beam misalignment caused by the varying posture of handheld terminals, highlighting the need for real-time beamforming strategies that dynamically adapt to posture changes. In multi-satellite DB, a critical challenge is the phase difference between signals transmitted by multiple satellites due to imperfect phase pre-compensation. This issue disrupts the coherence of signals from multiple satellites and significantly reduces the beamforming gain, emphasizing the need for advanced multi-antenna spatial reception techniques to mitigate these effects.

### 3.5. Quantitative analyses and balanced approaches

To achieve the vision of mobile satellite Internet, extensive engineering efforts and industry initiatives have been undertaken to foster innovation. AST SpaceMobile's experimental satellite BlueWalker 3 set a transmission rate record of 14 megabits per second (Mbps) in September 2023 for DTC services [22]. Subsequently, SpaceX successfully completed tests across various scenarios and Internet applications, achieving a DTC transmission rate of 17 Mbps [40]. In the following, we quantitatively evaluate the impact of key enabling technologies on the satellite–terrestrial link capacity of existing mobile smartphones, using parameter settings derived from AST SpaceMobile and Starlink V2 Mini DTC, as shown in Table 1 [41–43].

**Table 1**
Specific parameters in AST SpaceMobile and Starlink V2 Mini DTC.

| Satellite system | Regime | EIRP (dBW) | UT $G/T$ (dB·K$^{-1}$) | Carrier frequency (GHz) | Bandwidth (MHz) | Orbit height (km) | Array area (m$^2$) | UT type | Service | Test DL rate (Mbps) |
|---|---|---|---|---|---|---|---|---|---|---|
| AST SpaceMobile [41] | LEO | 46.46 | −36.6 | 0.892 | 4 | 515 | 64.00 | Handheld terminal | DTC | 14 |
| Starlink V2 Mini DTC [42,43] | LEO | 51.79 | −36.6 | 1.992 | 5 | 350 | 8.93 | Handheld terminal | DTC | 17 |

Considering that contemporary mobile satellite Internet systems are typically built upon 4G/5G cellular frameworks, we simulate satellite to ground transmission rate through three steps: ① calculating the received signal-to-noise ratio (SNR) based on the link budget; ② selecting an appropriate MCS level with a specific demodulation threshold that meets the reliability performance from the protocol-defined MCS tables [18]; and ③ simulating the satellite-to-ground transmission rate based on specific parameters in different mobile satellite Internet systems. We adopt the default MCS table (Table 5.1.3.1-1 in Ref. [18]) specified by the 5G new radio (NR) [18]. To account for specific satellite to ground impairments, we reserve a sufficient link margin to mitigate the impairments caused by atmospheric absorption, rain and cloud attenuation, scintillation, multipath fading, feeder loss, antenna pointing errors, and so on [5,6].

It should be noted that the simulated theoretical rate calculated from the link budget in Eq. (1) represents the baseband rate, including overhead such as physical layer pilots and the higher-layer protocol stack, whereas the test rates in Refs. [22,40] represent the net data rate excluding the above overhead. Therefore, it is valid that the theoretical rates exceed the test values at high elevation angles. The test rates that fall with the range of the simulated rates validate the reasonability of the link budget formula.

To quantitatively evaluate the impact of ELAAs on the satellite–terrestrial link capacity, we plot the DL transmission rate versus the array area of payloads with the elevation angles of 20°, 45°, and 90°, as shown in Fig. 3(a). It can be observed that doubling the antenna aperture area of the payload's ELAA yields a 3 dB increase in EIRP, which consequently increases the DL transmission rates of AST SpaceMobile and Starlink V2 Mini DTC by 3 and 4 Mbps, respectively. Notably, when the array area of the Starlink V2 Mini DTC reaches 14 m$^2$, its transmission rate becomes saturated, constrained by the maximum spectral efficiency of the MCSs. As for the MSCT, we consider a dual satellite cooperative transmission scenario in which two co orbiting satellites are separated by 3°, as seen from Earth center. As depicted in Fig. 3(b), we compare the DL transmission rate for different multi-satellite cooperative schemes with an equal total bandwidth. Compared with the single satellite baseline, the MC and DB schemes yield relative increases in DL rates of 49% and 76% for AST SpaceMobile and improvements of 44% and 69% for the Starlink V2 Mini DTC, respectively. It is worth noting that, when the elevation angle surpasses 40° for AST SpaceMoblie and 30° for the Starlink V2 Mini DTC, the DL rate under the DB scheme stagnates because the MCS attains its maximum spectral efficiency. This suggests that additional increases in bandwidth or the adoption of higher order MCS levels are necessary for the DB scheme to achieve further rate increases. Furthermore, for the Starlink V2 Mini DTC operating at an orbital altitude of just 350 km, an adjacent satellite's elevation angle is limited to 44° when the primary satellite is at zenith. Consequently, the DL rate under the MC scheme degrades at high elevation angles. In contrast, the DB scheme, thanks to its better power aggregation capability, can continue employing the highest MCS level at elevated angles, thereby preserving stable transmission rates. The relationship between the satellite-to-ground DL transmission rate and the UT elevation angle is also illustrated in Fig. 3(b). Higher elevation angles, which correspond to shorter satellite to ground distances, yield a significant increase in the DL transmission rate. Finally, we plot the DL transmission rate versus UT $G/T$ with the elevation angles of 20°, 45°, and 90°, as shown in Fig. 3(c). The simulation results demonstrate that, by combining beamforming techniques using sub-6 GHz MIMO cellular antennas and optimizing the single-antenna radiation pattern, a theoretical gain of at least 6 dB in $G/T$ can be achieved; this in turn increases the DL transmission rates of AST SpaceMobile and Starlink V2 Mini DTC by a maximum of 7.2 and 7.5 Mbps, respectively.

Aiming at existing mobile satellite Internet systems (i.e., AST SpaceMobile and Starlink V2 Mini DTC), we propose a staged and

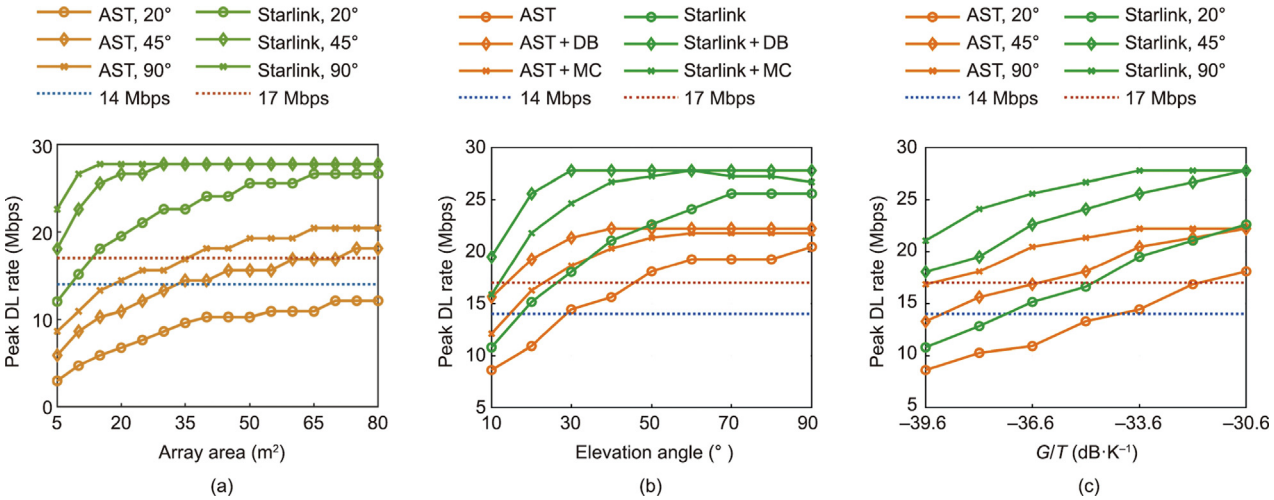


**Fig. 3.** DL transmission rate comparison with different key enabling technologies: (a) ELAA, (b) MSCT, and (c) UT antenna.

balanced optimization strategy based on key enabling technologies, while accounting for current engineering capabilities. From an implementation cost standpoint, optimizing UT capabilities should be the foremost direction of technological advancement. Nevertheless, the limited physical size of handheld terminals, combined with the half wavelength constraint for antenna design, imposes a strict upper bound on the number of internally integrated antennas, thereby constraining the maximum array gain. Under the spectrum-sharing framework of integrated satellite–terrestrial networks, UTs can reuse existing sub-6 GHz MIMO cellular antennas for beamforming to increase the effective gain. This approach complements ongoing efforts to optimize single antenna performance and avoids spatial conflicts arising from the integration of dedicated satellite antennas. In parallel, real-time beam calibration algorithms [44] should be developed to compensate for beam misalignment caused by the varying posture of handheld terminals and the high-speed movement of satellites, thereby maintaining link stability.

Under the constraints of engineering capabilities, enlarging the array aperture inevitably increases a satellite's volume, weight, and cost. Once the limits of manufacturing capacity are surpassed, costs escalate sharply to prohibitive levels. Moreover, interference with terrestrial services, as quantified by the PFD metric, imposes stringent limits on the EIRP capability of ELAAs. Accordingly, ELAA design must be driven by the transmission rate requirements of mobile satellite Internet while remaining within the bounds set by cost, interference, and UT capability. Furthermore, advanced ELAA enabled techniques such as beamforming [23,24], resource allocation [26], and mobility management techniques [27] can be exploited to further increase ELAA efficiency.

Constrained by engineering capabilities and costs, the performance targets of mobile satellite Internet may remain unattainable, even with optimized antenna design of UTs and payloads. This necessitates the adoption of MSCT to further expand system capacity. However, the implementation of MSCT is constrained by technological maturity. Leveraging the successful application of CA [32,33] and MC [34] technologies in cellular mobile communication systems, a preliminary MC-based cooperative transmission scheme for multiple satellites can be implemented to enable power aggregation across satellites. With the maturity of DB technology with imperfect CSI, the cooperative framework can evolve into a DB-based scheme for stronger power aggregation capability, trading off between technological maturity and performance requirements.

## 4. Conclusions

Beginning with the mathematical foundations of satellite communications, this paper examined advancements in payloads, terminals, frequency bands, and orbits, highlighting improvements in satellite-to-ground link capacity while acknowledging persistent fundamental limitations. By exploring the intricate relationships between satellite communication parameters and transmission capacity, critical enabling technologies were identified (i.e., ELAAs, mobility management, MSCT, and terminal antenna design), each offering distinct advantages and challenges. This comprehensive review not only reflects on past engineering achievements but also provides insights for mobile satellite communication systems.

## CRediT authorship contribution statement

**Wenjin Wang:** Methodology, Conceptualization, Writing – original draft. **Yiming Zhu:** Investigation, Formal analysis, Writing – original draft. **Yafei Wang:** Investigation, Formal analysis, Writing – original draft. **Rui Ding:** Writing – review & editing. **Symeon Chatzinotas:** Writing – review & editing.

## Declaration of competing interest

The authors declare that they have no known competing financial interests or personal relationships that could have appeared to influence the work reported in this paper.

## Acknowledgment

This work was supported in part by the National Key Research and Development Program of China (2023YFB2904703).

## References

[1] Braun TM. Satellite communications payload and system. 2nd ed. Hoboken: John Wiley & Sons; 2021.
[2] Ericsson joins MSSA to advance a non-terrestrial network ecosystem and expand global connectivity [Internet]. Stockholm: Ericsson; 2024 Sep 17 [cited 2024 Dec 6]. Available from: https://www.ericsson.com/en/news/2024/9/ericsson-joins-mssa-to-advance-a-non-terrestrial-network-ecosystem.
[3] Al Homssi B, Al-Hourani A, Wang K, Conder P, Kandeepan S, Choi J, et al. Next generation mega satellite networks for access equality: opportunities, challenges, and performance. IEEE Commun Mag 2022;60(4):18–24.
[4] Wall M. SpaceX completes 1st Starlink direct-to-cell constellation with launch from California [Internet]. New York City: Future US, Inc.; [updated 2024 Dec 5; cited 2025 Jun 28]. Available from: https://www.space.com/space-exploration/launches-spacecraft/spacex-launches-20-starlink-satellites-to-orbit-from-california.
[5] Maral G, Bousquet M, Sun Z. Satellite communications systems: systems, techniques and technology. 6th ed. Hoboken: John Wiley & Sons; 2020.
[6] Pratt T, Allnutt JE. Satellite communications. 3rd ed. Hoboken: John Wiley & Sons; 2019.
[7] Wu Y, Xiao L, Zhou J, Feng M, Xiao P, Jiang T. Large-scale MIMO enabled satellite communications: concepts, technologies, and challenges. IEEE Commun Mag 2024;62(8):140–6.
[8] International Telecommunication Union (ITU). Equivalent power-flux density limits examination. In: Proceedings of the ITU World Radiocommunication Seminar; 2024 Dec 2–6; Geneva, Switzerland. Geneva: International Telecommunication Union (ITU); 2024.
[9] Belostotski L, Jagtap S. Down with noise: an introduction to a low-noise amplifier survey. IEEE Solid-State Circuit Mag 2020;12(2):23–9.
[10] Zhang Z. Antenna design for mobile devices. 2nd ed. Hoboken: John Wiley & Sons; 2017.
[11] TR 38.821: Solutions for NR to support non-terrestrial networks (NTN). 3GPP standard. Valbonne: 3rd Generation Partnership Project (3GPP); 2023.
[12] Shang B, Wang Z, Li X, Yang C, Ren C, Zhang H. Spectrum sharing in satellite–terrestrial integrated networks: frameworks, approaches, and opportunities. 2025. arXiv:250102750.
[13] Lee HW, Medles A, Chen CC, Wei HY. Feasibility and opportunities of terrestrial network and non-terrestrial network spectrum sharing. IEEE Wirel Commun 2023;30(6):36–42.
[14] Zhang C, Jiang C, Kuang L, Jin J, He Y, Han Z. Spatial spectrum sharing for satellite and terrestrial communication networks. IEEE Trans Aerosp Electron Syst 2019;55(3):1075–89.
[15] Heydarishahreza N, Han T, Ansari N. Spectrum sharing and interference management for 6G LEO satellite–terrestrial network integration. IEEE Commun Surv Tutor. In press.
[16] Lee HW, Chen CC, Liao CIS, Medles A, Lin D, Fu IK, et al. Interference mitigation for reverse spectrum sharing in B5G/6G satellite–terrestrial networks. IEEE Trans Veh Technol 2024;73(3):4247–63.
[17] Demmer D, Zakaria R, Doré JB, Gerzaguet R, Ruyet DL. Filter-bank OFDM transceivers for 5G and beyond. In: Proceedings of the 2018 52nd Asilomar Conference on Signals, Systems, and Computers; 2018 Oct 28–31; Pacific Grove, CA, USA. New York City: IEEE; 2018. p. 1057–61.
[18] TS 38.214: Physical layer procedures for data. 3GPP standard. Valbonne: 3rd Generation Partnership Project (3GPP); 2019.
[19] Wang W, Chen T, Ding R, Seco-Granados G, You L, Gao X. Location-based timing advance estimation for 5G integrated LEO satellite communications. IEEE Trans Veh Technol 2021;70(6):6002–17.
[20] Wang W, Tong Y, Li L, Lu A, You L, Gao X. Near optimal timing and frequency offset estimation for 5G integrated LEO satellite communication system. IEEE Access 2019;7:113298–310.
[21] Balanis CA. Antenna theory: analysis and design. 3rd ed. Hoboken: John Wiley & Sons; 2005.
[22] AST SpaceMobile achieves space–based 5G cellular broadband connectivity from everyday smartphones [Internet]. Washington, DC: SpaceNews; 2023 Sep 20 [cited 2025 Jun 28]. Available from: https://spacenews.com/ast-spacemobile-achieves-space-based-5g-cellular-broadband-connectivity-from-everyday-smartphones/.

[23] Ha VN, Nguyen DHN, Duncan JCM, Gonzalez-Rios JL, Vásquez Peralvo JA, Eappen G. User-centric beam selection and precoding design for coordinated multiple-satellite systems. In: Proceedings of the IEEE 35th International Symposium on Personal, Indoor and Mobile Radio Communications; 2024 Sep 2–5; Valencia, Spain. New York City: IEEE; 2024.
[24] You L, Li KX, Wang J, Gao X, Xia XG, Ottersten B. Massive MIMO transmission for LEO satellite communications. IEEE J Sel Areas Commun 2020;38(8):1851–65.
[25] Ding F, Bao C, Zhou D, Sheng M, Shi Y, Li J. Towards autonomous resource management architecture for 6G satellite–terrestrial integrated networks. IEEE Netw 2024;38(2):113–21.
[26] Jia H, Wang Y, Peng H, Li W. Dynamic beam hopping and resource allocation for non-uniform traffic demand in NGSO satellite communication systems. IEEE Trans Veh Technol 2024;74(1):816–30.
[27] Ji S, Zhou D, Sheng M, Li J, Han Z. Dynamic space–ground integrated mobility management strategy for mega LEO satellite constellations. IEEE Trans Wirel Commun 2024;23(9):11043–60.
[28] Giordani M, Zorzi M. Non-terrestrial networks in the 6G era: challenges and opportunities. IEEE Netw 2020;35(2):244–51.
[29] Xu Z, Chen G, Fernandez R, Gao Y, Tafazolli R. Enhancement of direct LEO satellite-to-smartphone communications by distributed beamforming. IEEE Trans Veh Technol 2024;73(8):11543–55.
[30] Xiang Z, Gao X, Li KX, Xia XG. Massive MIMO downlink transmission for multiple LEO satellite communication. IEEE Trans Commun 2024;72(6):3352–64.
[31] Bacci G, De Gaudenzi R, Luise M, Sanguinetti L, Sebastiani E. Formation-of-arrays antenna technology for high-throughput mobile nonterrestrial networks. IEEE Trans Aerosp Electron Syst 2023;59(5):4919–35.
[32] Kibria MG, Lagunas E, Maturo N, Al-Hraishawi H, Chatzinotas S. Carrier aggregation in satellite communications: impact and performance study. IEEE Open J Commun Soc 2020;1:1390–402.
[33] TR 36.808: Carrier aggregation; base station (BS) radio transmission and reception. 3GPP standard. Valbonne: 3rd Generation Partnership Project (3GPP); 2013.
[34] TS 37.340: Evolved universal terrestrial radio access (E-UTRA) and NR; multi-connectivity; overall description; stage 2. 3GPP standard. Valbonne: 3rd Generation Partnership Project (3GPP); 2019.
[35] TR 36.819: Coordinated multi-point operation for LTE physical layer aspects. 3GPP standard. Valbonne: 3rd Generation Partnership Project (3GPP); 2013.
[36] Van Chien T, Mollen C, Bjornson E. Large-scale-fading decoding in cellular massive MIMO systems with spatially correlated channels. IEEE Trans Commun 2018;67(4):2746–62.
[37] Bjornson E, Sanguinetti L. Making cell-free massive MIMO competitive with MMSE processing and centralized implementation. IEEE Trans Wirel Commun 2019;19(1):77–90.
[38] Wang Y, Sun L, Du Z, Zhang Z. Antenna design for modern mobile phones: a review. Electromagn Sci 2024;2(2):1–36.
[39] Rao S, Wang Y. Shared-aperture design of the cellular antenna and satellite communication antenna with circular polarization in S-band for metal-bezel smartphones. IEEE Trans Antennas Propag 2024;72(5):3938–49.
[40] Kan M. SpaceX's cellular Starlink hits 17 Mbps download speed to Android phone [Internet]. New York City: PCMag; 2024 Mar 4 [cited 2025 Jun 28]. Available from: https://www.pcmag.com/news/spacexs-cellular-starlink-hits-17mbps-download-speed-to-android-phone.
[41] BlueWalker 3 non-geostationary satellite updated technical annex [Internet]. Washington, DC: Federal Communications Commission; 2021 Aug 31 [cited 2025 Apr 20]. Available from: https://apps.fcc.gov/els/GetAtt.html?id=281537&x=.
[42] Dempsey J. By electronic filing: GN docket No. 23-135 ICFS file No. SAT-MOD-20230207-00021 [Internet]. Washington, DC: Scribd; 2023 Nov 30 [cited 2025 Apr 20]. Available from: https://www.scribd.com/document/785956319/0cb9c344-f219-4b75-809b-d92a3e7451e7.
[43] Goldman D. Consolidated opposition to petitions and response to comments of SpaceX exploration holdings, LLC [Internet]. Washington, DC: Federal Communications Commission; 2023 May 30 [cited 2025 Jul 2]. Available from: https://www.fcc.gov/ecfs/document/10530137821424/1.
[44] Yu J, Liu X, Gao Y, Shen X. 3D on and off-grid dynamic channel tracking for multiple UAVs and satellite communications. IEEE Trans Wirel Commun 2021;21(6):3587–604.